Subband Transforms for Adaptive, RLS Direct Sequence Spread Spectrum Receivers

Stephan Berner and Phillip L. De Leon, *Senior Member, IEEE*

***Abstract*—Adaptive Direct Sequence Spread Spectrum (DSSS) receivers have advantages over their fixed matched filter counterparts including interference cancellation capabilities and simplification of PN code acquisition. However, convergence using the LMS algorithm will be very slow in situations with relatively high SNR and/or a large number of users. The use of the RLS algorithm will improve convergence speed but at significantly increased computational cost, especially for long PN codes. Unfortunately, computationally efficient, fast RLS algorithms cannot be used because the filter is updated at the symbol rate rather than at every sample. In this paper, we propose a subband version of the RLS-based receiver that utilizes multiple, shorter length adaptive filters. This approach significantly reduces computation and introduces architectural parallelism into the system implementation. We design an optimal subband transform and provide simulation results demonstrating the improved convergence properties as compared with the fullband system.**

***Index Terms*—Adaptive direct sequence spread spectrum, parallel receiver, subband transforms.**

I. Introduction

ADAPTIVE, direct sequence spread spectrum (DSSS) digital receivers have several advantages over their fixed matched filter counterparts [1]. These advantages include the ability to minimize the effects of multiuser interference (MUI), narrowband interference (NBI), and intersymbol interference (ISI) without having information about the channel or interferers. Another advantage of this receiver is that it requires no information about the pseudo-noise (PN) code, other than its length and, thus, does not require a code-acquisition phase. It does, however, require a training period.

In the fractionally spaced (FS) adaptive DSSS receiver illustrated in Fig. 1, a received baseband signal $x(n)$, which is the sum of a desired component and interference, is passed through the adaptive filter $\mathbf{w}$. The adaptive filter length L is equal to the PN code length times the number of samples per chip. The filter output is sampled at the symbol rate T_s and compared with a known training sequence $d(n)$. The resulting difference or error $e(n)$ is used to adjust the filter coefficients. After a training period, the coefficient vector is an approximation of the pulse-shaped PN sequence (if the interference is moderate) and may be fixed or updated in decision-directed mode.

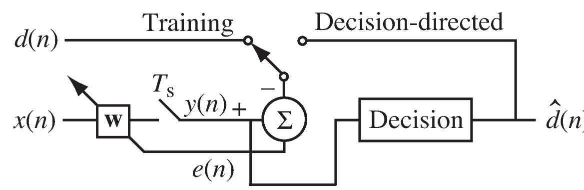

Fig. 1. Fractionally spaced adaptive DSSS receiver.

The input correlation matrix $\mathbf{R}$ (assuming uncorrelated symbols and no interference) is the outer product of the spreading sequence $[s_1, s_2 \ldots s_L]^T$ with itself plus a diagonal matrix $\sigma^2\mathbf{I}$, representing zero mean, σ^2 variance, additive white Gaussian noise (AWGN). Mathematically, the correlation matrix is given by

$$\mathbf{R} = \begin{bmatrix} s_1 \\ s_2 \\ \vdots \\ s_L \end{bmatrix} [\, s_1 \quad s_2 \quad \ldots \quad s_L \,] + \sigma^2\mathbf{I} \tag{1}$$

which has eigenvalues $\{s_1^2 + s_2^2 + \cdots + s_L^2 + \sigma^2, \sigma^2, \ldots, \sigma^2\}$. The eigenvalue spread is

$$\frac{\lambda_{\max}}{\lambda_{\min}} = \frac{s_1^2 + s_2^2 + \cdots + s_L^2 + \sigma^2}{\sigma^2} \tag{2}$$

which can be very large if the noise level is low. Such ill-conditioning will lead to slow convergence of the LMS adaptive filter which will be a problem in a changing environment. Using the recursive least squares (RLS) algorithm will improve convergence speed but at significantly increased computational cost [$O(L^2)$], especially in the case of long PN codes; fast RLS algorithms cannot be used because the filter is updated at the symbol rate rather than at every sample [1]. The observation that the convergence time for LMS-based adaptive DSSS receivers grows exponentially in the number of users, whereas for RLS, convergence time grows linearly [1], is also of interest.

In this paper, we turn our attention to the RLS-based receiver and propose a novel subband, adaptive DSSS receiver for three reasons. First, a subband receiver may potentially yield a lower bit error rate (BER) for a fixed training or convergence time. Second, shorter subband RLS adaptive filters will converge faster and require less computation than the longer, fullband equivalent [2]. A faster convergence rate will directly translate into a reduced training period for the receiver. Third, the subband transform will introduce parallelism into the architecture that opens up the possibility of a high-speed receiver implementation using relatively low-speed hardware. This approach for

Manuscript received December 19, 2003; revised November 24, 2004. This work was supported by NASA under Grant NAG 5-9323. The associate editor coordinating the review of this manuscript and approving it for publication was Dr. Yuan-Pei Lin.

S. Berner is a consultant located at 6518 Rita Ave., Apt. H, Huntington Park, CA 90255 USA (e-mail: sberner3@yahoo.com).

P. L. De Leon is with the Klipsch School of Electrical and Computer Engineering, New Mexico State University, Las Cruces, NM 88003-8001 (e-mail: pdeleon@nmsu.edu).

Digital Object Identifier 10.1109/TSP.2005.855111

introducing architectural parallelism has already been exploited in binary phase shift keying (BPSK), quaternary phase shift keying (QPSK), and quadrature amplitude modulation (QAM) receiver implementations with actual single-chip, 1.2-Gbps receivers utilizing 125-MHz CMOS technology, which has been reported in [3] and [4].

The remainder of this paper is organized as follows. In Section II, we describe the design of the subband, adaptive DSSS receiver and comment on the advantages of the potential parallel implementation. In Section III, we design and analyze an optimal subband transform based on a criterion of minimizing the BER. In Section IV, we provide simulation results, demonstrating the reduced BERs and faster convergence times. We also include other subband adaptive DSSS receivers that use the Discrete Cosine Transform (DCT) and Hadamard transform as their subband transform. As will be shown, these transforms perform nearly optimally but at reduced cost, especially in the case of the Hadamard transform, which has a very simple VLSI implementation. Finally, in Section V, we give our conclusions.

II. Subband, Adaptive DSSS Receiver Architecture

A. Proposed Subband Receiver

Subband adaptive filtering has been used in applications such as acoustic echo cancellation (AEC) in order to address the problems of slow convergence and high computational complexity associated with long adaptive filters [5]. One approach is to divide the fullband signal into multiple, lower rate subband signals that interfere (alias) as little as possible with each other. High-order analysis filters, oversampling, and adaptive cross filters can all be employed to minimize aliasing effects. Oversampled subbands are typically used in the AEC application since subband aliasing severely limits echo cancellation performance [6]. In another approach, the subband signals are not downsampled, but rather, a parallel set of adaptive sparse subfilters is utilized [7]. With the subband technique, convergence time and computational complexity can be reduced.

In digital communications, the situation is quite different. Most important in the adaptive DSSS receiver are the sampling at the symbol time of the receiver output and the update of the adaptive filter at the symbol rate [1]. The performance measure of interest is the BER rather than the mean-square error (MSE) or other standard adaptive filter measures. Furthermore, details about the received signal such as the spreading sequence and pulse shaping are known, as compared with the situation in AEC, where the input speech signal can only be described statistically. We can exploit this knowledge to design an adaptive DSSS receiver that uses a subband transformation but in a manner that is much simpler than conventional subband adaptive filtering architectures [8].

In the proposed subband, adaptive DSSS receiver illustrated in Fig. 2, the received signal $x(n)$ is partitioned into length-M windows and decomposed by a linear transformation $\mathbf{T}$ into M lower rate (subband) signals $x_1, \ldots, x_M$ [8]. It is assumed that the number of input samples belonging to one symbol is a multiple of the window size M. The lower rate signals are passed through M subband adaptive filters $\mathbf{w}_1, \ldots, \mathbf{w}_M$ (each shorter than in the fullband case and updated at the symbol rate) and the outputs $y_1, \ldots, y_M$ are sampled at the symbol rate T_s. The resulting signals $u_1, \ldots, u_M$ are scaled by gain factors $\alpha'_1, \ldots, \alpha'_M$ to yield $v_1, \ldots, v_M$. These signals are then applied to the inverse transformation $\mathbf{T}^{-1}$ and the first element picked off to yield z_1. We use z_1 to form $\hat{d}(n)$, which is the estimate of the transmitted symbol $d(n)$. We will establish criteria for the design of an optimal transform and the gain factors in the next section.

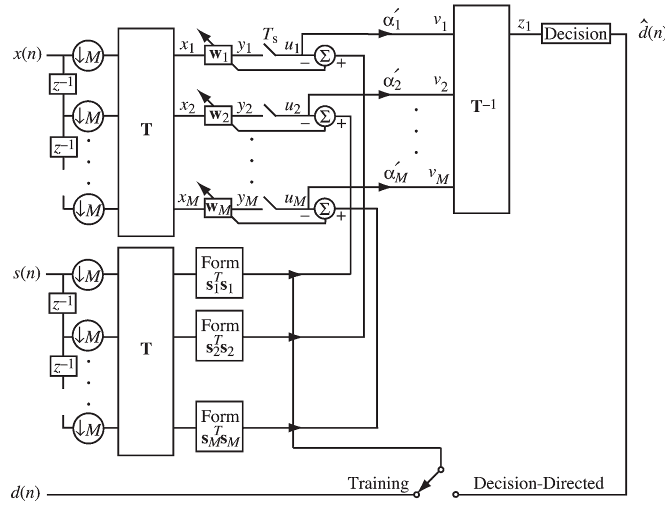

Fig. 2. Subband, adaptive DSSS receiver.

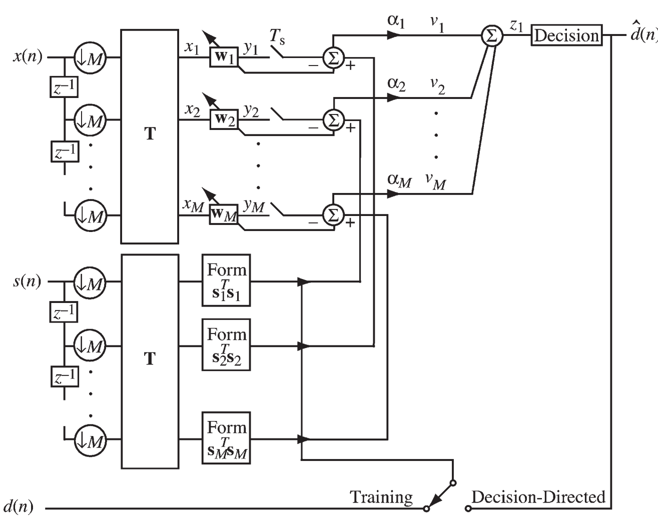

Fig. 3. Subband, adaptive DSSS receiver with further simplification (elimination of $\mathbf{T}^{-1}$).

We note that symbol rate sampling in the subbands is equivalent to sampling the output of $\mathbf{T}^{-1}$ (picking off the first element z_1) due to the fact that the length of one symbol is a multiple of M. Because of this sampling, much of the computation involved with $\mathbf{T}^{-1}$ can be eliminated since we only need z_1. Thus, if we scale the signals $v_1, \ldots, v_M$ by the corresponding elements of the first row of $\mathbf{T}^{-1}$ or, equivalently, let $\alpha_m = \alpha'_m[\mathbf{T}^{-1}]_{1,m}$, the inverse transform block $\mathbf{T}^{-1}$ in Fig. 2 can be replaced by a simple summation, as in Fig. 3. As can be seen in Fig. 3, the synthesis side of the proposed subband, adaptive DSSS receiver differs significantly from other subband-based applications [8].

The vector of desired subband signals is obtained in the following way. For the fullband receiver, the desired signal is the convolution of the oversampled, pulse-shaped PN sequence [weighted by the symbol $d(n)$] with the matched filter sampled at the symbol time. Alternatively, this desired signal is the inner product of the oversampled, pulse-shaped PN sequence with itself weighted by the symbol. For the subband receiver, the vector of desired subband signals is the inner product of the *subband* version of the PN sequence [$s(n)$ transformed by $\mathbf{T}$] with itself weighted by the symbol $d(n)$. This is shown in the lower left parts of Figs. 2 and 3.

B. Parallel System Implementation

One motivation for the subband receiver (in addition to computational and convergence issues) is to introduce architecture parallelism for implementation purposes. Since the subband adaptive filters are updated at the symbol rate in exactly the same way as the fullband receiver, a simple polyphase implementation of the adaptive filter in the fullband receiver would provide equivalent parallelism but no reduction in computational complexity. However, the subband receiver can reduce the requirements of the delay lines associated with the filters. In the fullband receiver of Fig. 1, we have a single, long adaptive filter (possibly implemented in polyphase form), and the associated delay line must operate at the high input sample rate. In the receiver that has M subbands (Fig. 3), however, only M delay elements need to operate at the higher rate since the delay lines associated with the filters operate at $1/M$ times the input sample rate. For a long filter or, equivalently, a high spread-spectrum processing gain, this implementation advantage can be significant.

III. Optimal Transform Design for Minimum BER

A. Optimization Criteria

A common assumption about the error signal of an adaptive filter is that it is white Gaussian noise after convergence [1]. Therefore, the MSE after convergence is directly related to the BER. In order to understand the effect of the subband transform on BER, we could calculate the minimum MSE (MMSE) at the receiver output using a general transform and arbitrary input autocorrelations. As it turns out, the MMSE derived in this way is not too useful for purposes of optimizing the transform for minimum error because it is a complicated rational function involving the elements of the transformation matrix [9]. As an indirect method toward minimizing the BER, we consider calculating a lower bound on the receiver's output SNR (assuming subband matched filters) and designing $\mathbf{T}$ to maximize this bound. Later in this section, we will discuss the relation between maximizing the lower bound and the actual SNR.

B. Additive White Gaussian Noise Case

We begin the transform design by assuming a single user with AWGN (zero mean, σ^2 variance) and subband matched filters (since we have AWGN); for purposes of transform design, we do not consider interference but do include it in our simulation results. With L denoting the number of samples per symbol, we assume that the subband filters are of integer length $N = L/M$. We also assume in this analysis that the gain factors α_m are fixed. We partition the oversampled and pulse-shaped spreading sequence into vectors of length M, which form the columns of

$$\mathbf{S} = \begin{bmatrix} s_1 & s_{M+1} & \cdots & s_{(N-1)M+1} \\ s_2 & s_{M+2} & \cdots & s_{(N-1)M+2} \\ \vdots & \vdots & \vdots & \vdots \\ s_M & s_{2M} & \cdots & s_{NM} \end{bmatrix}. \tag{3}$$

The subband spreading sequences are then given by

$$\mathbf{S}_{\text{sub}} = (\mathbf{TS})^T = [\mathbf{s}_1 \mid \mathbf{s}_2 \mid \ldots \mid \mathbf{s}_M] \tag{4}$$

where $\mathbf{s}_m$ is the mth subband spreading sequence. Referring to Fig. 3, the received signal is given by

$$\mathbf{x} = d \begin{bmatrix} s_1 \\ s_2 \\ \vdots \\ s_L \end{bmatrix} + \sigma \begin{bmatrix} n_1 \\ n_2 \\ \vdots \\ n_L \end{bmatrix} = d\mathbf{s} + \sigma\mathbf{n} \tag{5}$$

where d is the data bit (either $+1$ or -1), $\mathbf{s}$ is the spreading sequence, and $\mathbf{n}$ is the noise.

We first compute the signal power by considering only the signal component $d\mathbf{s}$ of (5). After filling the delay line, passing through the transform $\mathbf{T}$ and subband matched filters, and scaling by α_m, we have

$$v_m^{\text{s}} = d\alpha_m \mathbf{s}_m^T \mathbf{s}_m \tag{6}$$

where

$$\mathbf{s}_m = \begin{bmatrix} t_{m,1}s_1 + t_{m,2}s_2 + \cdots + t_{m,M}s_M \\ t_{m,1}s_{M+1} + t_{m,2}s_{M+2} + \cdots + t_{m,M}s_{2M} \\ \vdots \\ t_{m,1}s_{(N-1)M+1} + t_{m,2}s_{(N-1)M+2} + \cdots + t_{m,M}s_{NM} \end{bmatrix} \tag{7}$$

and $t_{i,j}$ is the i,jth element of $\mathbf{T}$. The signal power is then given by

$$P_{\text{s}} = \left(\sum_{m=1}^{M} v_m^{\text{s}} \right)^2. \tag{8}$$

Next, we compute the noise power by considering only the noise component $\sigma\mathbf{n}$ of (5). In this case, (6) becomes

$$v_m^{\text{n}} = \sigma\alpha_m \mathbf{n}_m^T \mathbf{s}_m \tag{9}$$

where

$$\mathbf{n}_m = \begin{bmatrix} t_{m,1}n_1 + t_{m,2}n_2 + \cdots + t_{m,M}n_M \\ t_{m,1}n_{M+1} + t_{m,2}n_{M+2} + \cdots + t_{m,M}n_{2M} \\ \vdots \\ t_{m,1}n_{(N-1)M+1} + t_{m,2}n_{(N-1)M+2} + \cdots + t_{m,M}n_{NM} \end{bmatrix}. \tag{10}$$

The noise power is then given by

$$P_{\text{n}} = E\left[\left(\sum_{m=1}^{M} v_m^{\text{n}} \right)^2 \right] \tag{11}$$

where E is the expectation operator, and v_m^{n} is given in (9). The output SNR is then the ratio of (8) to (11)

$$\mathrm{SNR} = \frac{P_{\mathrm{s}}}{P_{\mathrm{n}}}. \tag{12}$$

In order to simplify, we assume the rows of $\mathbf{T}$ are orthogonal and that all elements of the spreading sequence and $\mathbf{T}$ are normalized. Then, $\mathbf{s}_m^T\mathbf{s}_m \leq NM^2$, and the cross-terms in (11) are zero, leaving

$$P_{\mathrm{n}} = E\left[\sum_{m=1}^{M} \left(v_m^{\mathrm{n}}\right)^2\right] \tag{13}$$

and

$$\mathrm{SNR} \geq \frac{\left(\sum\limits_{m=1}^{M} d\alpha_m \mathbf{s}_m^T \mathbf{s}_m\right)^2}{NM^2\sigma^2 \sum\limits_{m=1}^{M} \alpha_m^2 \sum\limits_{k=1}^{M} t_{m,k}^2}. \tag{14}$$

The problem is now to maximize this lower bound. If we constrain the denominator to be a constant, then we need only maximize the numerator. Because the data is assumed to be binary, the square in the numerator can be dropped in order to find the extrema.

We illustrate the solution to the problem for the simple case of a two-subband ($M = 2$) receiver with length-two ($N = 2$) subband filters—the general case is similarly solved. For this simple case, (14) becomes

$$\mathrm{SNR} \geq \frac{\left[d\alpha_1 \mathbf{s}_1^T \mathbf{s}_1 + d\alpha_2 \mathbf{s}_2^T \mathbf{s}_2\right]^2}{8\sigma^2\left[\left(t_{1,1}^2 + t_{1,2}^2\right)\alpha_1^2 + \left(t_{2,1}^2 + t_{2,2}^2\right)\alpha_2^2\right]}. \tag{15}$$

If we constrain the denominator in (15) to be a constant, then we need only maximize the numerator. Because the data is assumed to be binary, the square in the numerator can be dropped in order to find the extrema. Using the method of Lagrange multipliers, a sufficient condition for extrema is

$$\nabla_{\mathbf{t}} f - \lambda \nabla_{\mathbf{t}}\, g = \mathbf{0} \tag{16}$$

where

$$\mathbf{t} = \left[t_{1,1}\ t_{1,2}\ t_{2,1}\ t_{2,2}\right]^T \tag{17}$$

$$f = \alpha_1 \mathbf{s}_1^T \mathbf{s}_1 + \alpha_2 \mathbf{s}_2^T \mathbf{s}_2 \tag{18}$$

$$g = \alpha_1^2\left(t_{1,1}^2 + t_{1,2}^2\right) + \alpha_2^2\left(t_{2,1}^2 + t_{2,2}^2\right) \tag{19}$$

and λ is the multiplier. Equation (16) leads to

$$\begin{bmatrix} 2\alpha_1^2\mathbf{A}_1 & \mathbf{0} \\ \mathbf{0} & 2\alpha_2^2\mathbf{A}_2 \end{bmatrix} \mathbf{t} = \mathbf{0} \tag{20}$$

where

$$\mathbf{A}_i = \begin{bmatrix} \dfrac{s_1^2 + s_3^2}{\alpha_i} - \lambda & \dfrac{s_1 s_2 + s_3 s_4}{\alpha_i} \\ \dfrac{s_1 s_2 + s_3 s_4}{\alpha_i} & \dfrac{s_2^2 + s_4^2}{\alpha_i} - \lambda \end{bmatrix} \tag{21}$$

which can be rewritten as the following eigenvalue problem:

$$\mathbf{B}\mathbf{T}^T = \lambda \mathbf{T}^T \begin{bmatrix} \alpha_1 & 0 \\ 0 & \alpha_2 \end{bmatrix} \tag{22}$$

where

$$\mathbf{B} = \begin{bmatrix} s_1^2 + s_3^2 & s_1 s_2 + s_3 s_4 \\ s_1 s_2 + s_3 s_4 & s_2^2 + s_4^2 \end{bmatrix}. \tag{23}$$

Thus, the transform optimization problem can be solved by choosing the rows of $\mathbf{T}$ to be the eigenvectors of $\mathbf{B}$ and α_i to be the corresponding eigenvalue. For the general case of M subbands with subband filter lengths N, the elements of $\mathbf{B}$ are given by

$$b_{m,\mathrm{n}} = \sum_{i=1}^{M} s_{(i-1)M+m}\, s_{(i-1)M+\mathrm{n}}. \tag{24}$$

The algorithm for finding the optimal transformation matrix under the assumption of subband matched filters, which maximizes the lower bound in (14), can be summarized as follows. Build the matrix $\mathbf{B}$ with entries as in (24) using the spreading sequence that is assumed to be given. Find the eigenvectors of $\mathbf{B}$, use them as the rows of $\mathbf{T}$ (in any order), and set α_i to be the corresponding eigenvalues. Simulation results of the subband receiver using the optimized transform will be given in Section IV.

The optimized transform matrix $\mathbf{T}$ can be equivalently seen as an eigenvector decomposition of the average input correlation matrix, as seen by the parallel receiver. To illustrate, consider a simple case with $M = 3$ and $N = 4$, which implies a pulse-shaped spreading sequence of length 12 and 12 samples per symbol. $\mathbf{B}$ is a 3×3 matrix with diagonal entries [according to (24)]

$$\begin{aligned} b_{1,1} &= s_1^2 + s_4^2 + s_7^2 + s_{10}^2 \\ b_{2,2} &= s_2^2 + s_5^2 + s_8^2 + s_{11}^2 \\ b_{3,3} &= s_3^2 + s_6^2 + s_9^2 + s_{12}^2 \end{aligned} \tag{25}$$

and off-diagonal entries

$$\begin{aligned} b_{12} = b_{21} &= s_1 s_2 + s_4 s_5 + s_7 s_8 + s_{10} s_{11} \\ b_{13} = b_{31} &= s_1 s_3 + s_4 s_6 + s_7 s_9 + s_{10} s_{12} \\ b_{23} = b_{32} &= s_2 s_3 + s_5 s_6 + s_8 s_9 + s_{11} s_{12}. \end{aligned} \tag{26}$$

The input correlation matrix $\mathbf{R}$ in this case is a 12×12 matrix, which can be partitioned into 3×3 blocks as follows:

$$\mathbf{R} = \left[\begin{array}{c|c|c|c} \mathbf{R}_1 & & & \\ \hline & \mathbf{R}_2 & & \\ \hline & & \mathbf{R}_3 & \\ \hline & & & \mathbf{R}_4 \end{array}\right]. \tag{27}$$

It can be seen that the matrix $\mathbf{B}$ is the sum of these diagonal blocks $\mathbf{B} = \sum_i \mathbf{R}_i$ or an *average* input correlation matrix.

At the extreme of scaling when $M = L$, the subband filters have length one, and we essentially have a fullband receiver. In this case, $\mathbf{B} = \mathbf{R}$, and the optimal transform result is equivalent to the well-known eigenfilter result, which maximizes the SNR [2].

One open question is the relation between the lower bound of the output SNR, which was maximized, and the true SNR.

A numerical evaluation of the exact SNR given in (12) for different transformation matrices $\mathbf{T}$ reveals that the matrix optimized with the method above does, in fact, lead to the maximum SNR value [9].

C. On the Existence of the Optimal Transform

The matrix $\mathbf{B} = \mathbf{S}\mathbf{S}^T$, and therefore, $\text{rank}(\mathbf{B}) = \min(N, M)$. Alternatively, $\mathbf{B}$ ($N \times N$) can be full rank only if $N \geq M$. This can be seen by again thinking of $\mathbf{B}$ as an average input correlation matrix $\mathbf{B} = \sum \mathbf{R}_i$ and with help of the following well-known rank inequality [10]

$$\text{rank}(\mathbf{F} + \mathbf{G}) \leq \text{rank}(\mathbf{F}) + \text{rank}(\mathbf{G}). \tag{28}$$

Here, if the length of the subband filter N is greater than or equal to the transform size M, then the matrix $\mathbf{B}$ is typically nonsingular (based on our observations) with M distinct eigenvalues; if $N < M$, there are usually N distinct nonzero eigenvalues and $M - N$ zero eigenvalues (again, based on our observations). It may, however be possible to construct a spreading sequence such that $\mathbf{B}$ is singular for $N \geq M$. The nonzero eigenvalues are typically distinct; therefore, there exists a corresponding set of orthogonal eigenvectors; eigenvectors corresponding to the zero eigenvalues can be chosen arbitrarily. Therefore, in general, M orthogonal eigenvectors can be found, and an optimal transform $\mathbf{T}$ can be constructed as shown in the previous section.

IV. Results

The proposed RLS-based subband, adaptive DSSS receiver was simulated using the DCT, Hadamard transform, and optimal transform from Section III with various numbers of subbands. System parameters include a length-31 PN sequence and chip pulses shaped with a square-root raised cosine (SRRC) filter (50% excess bandwidth). In the fullband receiver, the adaptive filter length $L = 128$ (length-31 PN sequence, four samples per chip, which yields 124 samples, resampled to get 128 samples). In the subband receiver, subband adaptive filter lengths are $N = 32$, 16, and 8 for $M = 4$, 8, 16 subbands, respectively. We assume perfect carrier and chip synchronization. In addition, we initialize the gain factors to the eigenvalues of $\mathbf{B}$ but allow them to adapt based on $d - z_1$ (as in Fig. 3) since, depending on the noise or interference, the subband filters may adapt to something other than the subband matched filters. In this case, the transform derived in the previous section may be suboptimal. The update of the subband filters and the gain factors are independent of each other and can be viewed as two cascaded control loops.

A. Bit Error Rate Results

BER results for the subband receiver were compared to theory, the matched filter receiver, and the fullband receiver; for each simulation point, 2×10^5 symbols are used. For simulations involving MUI and NBI, we assume four other users and three narrowband interferences (sinusoids), respectively, where each is 6 dB stronger than the desired signal; zero mean, white Gaussian noise is also added to achieve a desired SNR, which, during training, is 6 dB. Comparison of BERs for the fullband and subband receivers is based on a fixed convergence time: We adjust the initial RLS parameters so that the number of subbands multiplied by the convergence time of the receiver is constant.

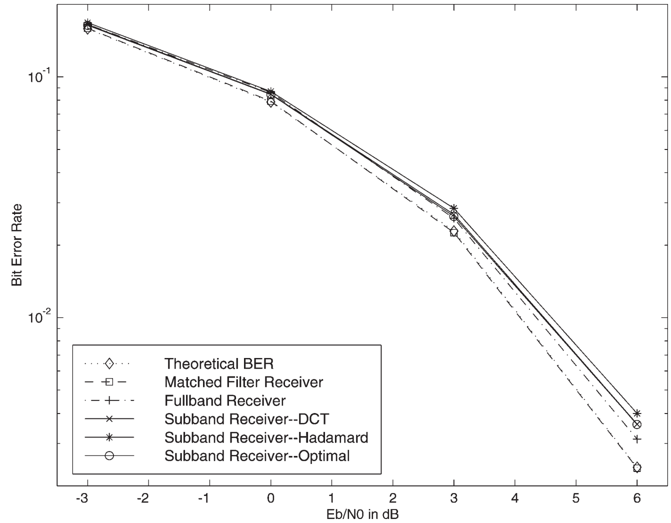

Fig. 4. BERs for the subband, adaptive DSSS receiver ($M = 4$ subbands, various transforms, RLS filters) in AWGN.

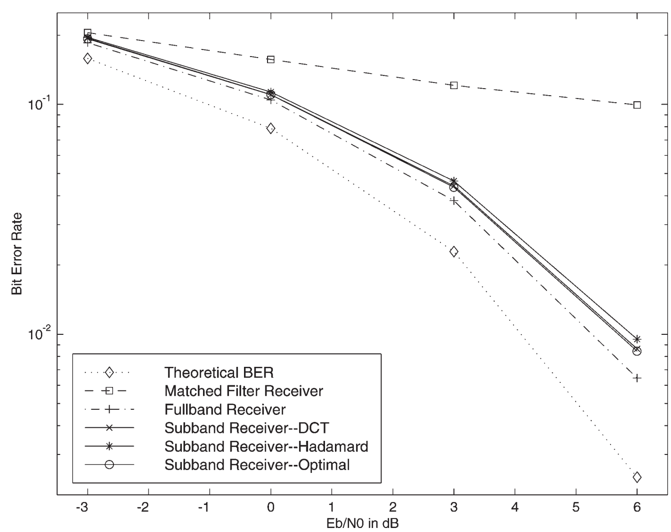

Fig. 5. BERs for the subband, adaptive DSSS receiver ($M = 4$ subbands, various transforms, RLS filters) in MUI and NBI.

Fig. 4 illustrates the BER curves for the various receivers in AWGN. As can be seen, the subband, adaptive receivers ($M = 4$ subbands) perform nearly as well as the fullband receiver but with significantly reduced computational complexity, a much faster convergence speed ($4\times$), and the added feature of a parallel implementation. The receiver with the optimal transform does in fact have a slightly better BER than that with the DCT and Hadamard transforms. However, given the simple implementation of these latter transforms, the designer may choose one of these instead. Fig. 5 illustrates the BER curves for the various receivers in MUI and NBI. For this case, the results are similar to the AWGN case, except for the matched filter receiver.

Figs. 6 and 7 elaborate upon the subband (DCT) adaptive DSSS receiver performance for various numbers of subbands. The results for the AWGN case (Fig. 6) show relatively good scaling of the architecture, with subband receivers performing

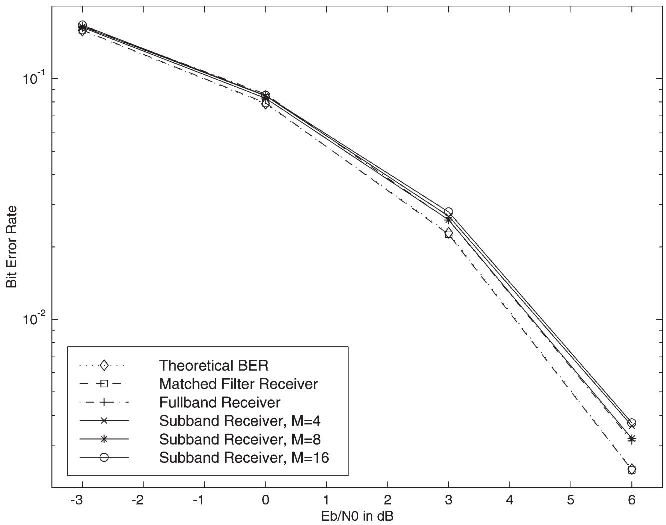

Fig. 6. BERs for the subband, adaptive DSSS receiver (various numbers of subbands, DCT, RLS filters) in AWGN.

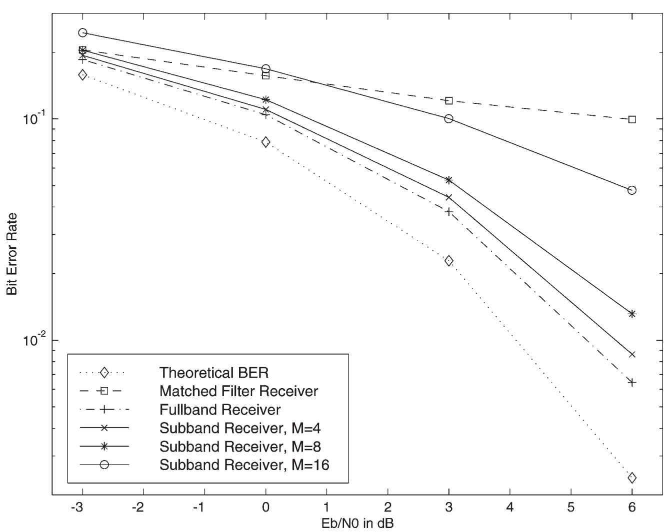

Fig. 7. BERs for the subband, adaptive DSSS receiver (various numbers of subbands, DCT, RLS filters) in MUI and NBI.

as well as the fullband receiver in all cases but, again, with reduced computational complexity [$O(L^2/M)$ and assuming a relatively small overhead associated with the transform] and a much faster convergence speed (increasing linearly with the number of subbands). For the MUI/NBI case (Fig. 7), the BER increases with increasing number of subbands in the receiver. The degradation in terms of E_b/N_0 is similar over the range shown.

B. Transform Results

Table I gives the MSE (actual values calculated from theory) of the receiver output for the MUI case where we have two interfering synchronous users, each 10 dB stronger than the desired user at 6 dB SNR. The results for the four-subband receiver show that the optimized transform derived for the AWGN case also performs slightly better than other transforms in the MUI case when using subband Wiener filters and equally well when using subband matched filters.

TABLE I
SUBBAND RECEIVER MSE WITH DIFFERENT TRANSFORMS (FOUR SUBBANDS) WITH 10 dB MUI, NO NBI

	Matched Subband Filters	Subband Wiener Solutions
Identity	0.5784	0.1781
Hadamard	0.5784	0.1432
DCT	0.5784	0.1360
Optimized	0.5784	0.1348

V. CONCLUSIONS

In this paper, we have proposed a subband version of the RLS-based, adaptive DSSS receiver. The resulting subband receiver is designed and operated differently than other subband adaptive systems such as acoustic echo cancelers because of the sampling at the symbol time of the receiver output and the update of the adaptive filter at the symbol rate. We have shown that the subband receiver, when using either the optimal transform, DCT, or Hadamard transform, has BERs comparable to the fullband receiver but with a faster convergence speed (and thus a reduced training period) and significantly reduced computation (fast RLS cannot be used in such a receiver). In addition, the inherent architectural parallelism may allow for high-speed system implementations. For spread-spectrum systems with long PN codes or many users, these are significant advantages. Although the subband receiver with the optimal transform was shown to give slightly better BERs, convenient implementations of the DCT or Hadamard transforms may yield a more practical subband receiver.

ACKNOWLEDGMENT

The authors wish to thank the anonymous reviewers for their helpful comments, which improved the quality of the paper.

REFERENCES

[1] S. Miller, "An adaptive direct-sequence code-division multiple-access receiver for multiuser interference rejection," *IEEE Trans. Commun.*, vol. 43, no. 2/3/4/, pp. 1746–1754, Feb./Mar./Apr. 1995.

[2] S. Haykin, *Adaptive Filter Theory*. Englewood Cliffs, NJ: Prentice-Hall, 1998.

[3] R. Sadr, P. P. Vaidyanathan, D. Raphaeli, and S. Hinedi, "Parallel Digital Modem using Multirate Digital Filter Banks," Jet Propulsion Lab., Pasadena, CA, Tech. Rep. 94-20, 1994.

[4] A. Gray, E. Satorius, and P. Ghuman, "All-digital architectures for implementation of a very high rate 16-QAM demodulator and receiver," in *Proc. ICSPAT*, 1999.

[5] A. Gilloire and M. Vetterli, "Adaptive filtering in subbands with critical sampling: Analysis, experiments, and applications to acoustic echo cancellation," *IEEE Trans. Signal Process.*, vol. 40, no. 8, pp. 1862–1875, Aug. 1992.

[6] P. De Leon and D. Etter, "Experimental results with increased bandwidth analysis filters in oversampled subband acoustic echo cancelers," *IEEE Signal Process. Lett.*, vol. 2, no. 1, pp. 1–3, Jan. 1995.

[7] M. Petraglia, R. Alves, and P. Diniz, "New structures for adaptive filtering in subbands with critical sampling," *IEEE Trans. Signal Process.*, vol. 48, no. 12, pp. 3316–3327, Dec. 2000.

[8] M. Petraglia and S. Mitra, "Adaptive FIR filter structure based on the generalized subband decomposition of FIR filters," *IEEE Trans. Circuits Syst. II*, vol. 40, no. 6, pp. 354–362, Jun. 1993.

[9] S. Berner, "Subband Transforms for Adaptive Direct Sequence Spread Spectrum Receivers with Application to Parallel Implementations," Ph.D. dissertation, New Mexico State Univ., Las Cruces, NM, 2001.

[10] R. Horn and C. Johnson, *Matrix Analysis*. New York: Cambridge Univ.Press, 1996.

Stephan Berner was born in Essen, Germany, in 1967. He received the Diplom Ingenieur (FH) degree from Fachhochschule Bochum, Abt. Gelsenkirchen, Gelsenkirchen, Germany, in 1990 and the Diplom Ingenieur degree from University of Bochum in 1993. He received the M.S. and Ph.D. degrees, in 1999 and 2001, respectively, both in electrical engineering, from New Mexico State University, Las Cruces.

From 1993 to 1995, he was an electrician with Reinders GmbH, Essen, and from 1995 to 1997, he was a hardware designer for radar signal acquisition and processing with Hope Electronics, Seoul, Korea. From 2000 to 2002, he was with the Rockwell Science Center, Thousand Oaks, CA, and from 2001 to 2002, he was with Valence Semiconductor, Irvine, CA. He currently works as a consultant.

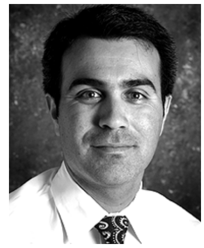

Phillip L. De Leon (SM'03) was born in San Antonio, TX, in 1967. He received the B.S. degree in electrical engineering and the B.A. degree in mathematics from the University of Texas, Austin, in 1989 and 1990, respectively. He received the M.S. and Ph.D. degrees in electrical engineering from the University of Colorado, Boulder, in 1992 and 1995, respectively.

In 1990, he was recipient of the AT&T Bell Laboratories Cooperative Research Fellowship for graduate study. After receiving the Ph.D. degree, he joined the Klipsch School of Electrical and Computer Engineering, New Mexico State University, Las Cruces, where he currently serves as an Associate Professor and Associate Director of the Center for Space Telemetering and Telecommunications. His research interests include adaptive, multirate, and speech signal processing; embedded systems, and wireless systems.

Dr. De Leon was the Finance Chair of the 2004 IEEE DSP/SPE Workshop and is a member of Eta Kappa Nu.